Infrared emission spectroscopy of NH: Comparison of a cryogenic echelle spectrograph with a Fourier transform spectrometer

R. S. Ram
Department of Chemistry, University of Arizona, Tucson, Arizona 85719

P. F. Bernath
Department of Chemistry, University of Arizona, Tucson, Arizona 85719 and Department of Chemistry, University of Waterloo, Waterloo, Ontario, N2L 3G1, Canada

K. H. Hinkle
Kitt Peak National Observatory, National Optical Astronomy Observatories, Tucson, Arizona 85726

(Received 9 November 1998; accepted 22 December 1998)

The high-resolution emission spectrum of NH has been observed in the near infrared using a Fourier transform spectrometer (FTS) and a cryogenic echelle spectrograph (called Phoenix) at the National Solar Observatory at Kitt Peak. By using a large format InSb array detector, the newly constructed Phoenix is calculated to offer a large increase in sensitivity over a Fourier transform spectrometer for measurements near 5 μm (2000 cm^{-1}). In order to test the performance of Phoenix, we recorded vibration–rotation emission spectra of the free-radical NH. The infrared bands of NH were produced in a microwave discharge of a mixture of NH_3 and He. The rotational structure of five bands, 1–0, 2–1, 3–2, 4–3, and 5–4 in the 2200–3500 cm^{-1} region has also been measured using two FTS spectra. An analysis of these bands combined with the previous electronic, vibration–rotation, and pure rotation measurements provides improved molecular constants for the ground electronic state. In particular, we have extended the range of measured J values so that the new constants are suitable for predicting line positions in high-temperature sources such as stellar atmospheres and flames. A comparison of the Phoenix spectra with the FTS spectra confirms the higher sensitivity of the Phoenix spectrometer. The relative advantages and disadvantages of instruments like Phoenix are discussed. Although designed for astronomical work, cryogenic echelle spectrographs have applications in the ultrasensitive detection of molecules in chemical physics. [S0021-9606(99)01412-9]

I. INTRODUCTION

NH is an extensively studied free-radical of fundamental importance. This radical was first detected in 1893 by Eder[1] through the observation of the $A\,^3\Pi - X\,^3\Sigma^-$ transition near 336 nm. This work was followed by numerous studies of the electronic spectra of NH from the visible to the vacuum ultraviolet. A more complete review of the previous work on electronic spectroscopy can be found in our previous papers.[2,3] Recent experimental[4–16] and theoretical[17–23] studies have been motivated by applications in astrophysics,[24–34] atmospheric science[35] and chemistry.[36–43]

There have been several infrared and far-infrared studies of NH aimed at extracting precise molecular and hyperfine constants in the ground state. Far-infrared laser magnetic resonance spectra have been observed by Radford and Litvak[44] and Wayne and Radford,[45] while the zero field pure rotational spectrum was measured by Heuval *et al.*[46] using a tunable far-infrared sideband laser spectrometer. Improved measurements of the $N=1\leftarrow 0$ transitions have recently been made with the Cologne terahertz spectrometer.[47]

The infrared spectra of this radical have also been studied by difference frequency spectroscopy,[48] matrix isolation spectroscopy,[49] and Fourier transform spectroscopy.[50–52] Bernath and Amano[48] have observed the fundamental 1–0 band with a difference frequency spectrometer, while Milligan and Jacox[49] observed the fundamental band by matrix isolation spectroscopy. Sakai *et al.*[50] and Green and Caledonia[51] have observed these bands at moderate resolution, while Boudjaadar *et al.*[52] measured the vibration–rotation bands up to $v=5-4$ in the ground state.

The high-resolution measurements of the $\Delta v=1$ vibrational bands of NH are important since they fall in the 3 μm atmospheric window. In fact, the $\Delta v=1$ vibration–rotation lines of NH were observed in the star α-Orionis[27] before the spectra were measured in a laboratory. Vibration–rotation lines of NH have also been detected in oxygen-rich and carbon-rich giant and supergiant stars.[29–31] Recently, the NH radical has been identified in the solar spectrum using the vibration–rotation[32] and pure rotation[33] lines.

In a previous publication, we reported on an analysis of the $A\,^3\Pi - X\,^3\Sigma^-$ transition of NH measured at high resolution using a Fourier transform spectrometer. In recent work, Morino and Kawaguchi[53] have made far-infrared absorption measurement of the NH, NH_2, NHD, and ND_2 radicals. Their NH measurements agreed to $\pm 0.000\,62$ cm^{-1} with the lines predicted using the constants from our analysis of the $A\,^3\Pi - X\,^3\Sigma^-$ transition.[3]

The deuterated molecule ND has also been studied in detail. The electronic spectra of ND were studied by several workers over the span of several decades.[54–58] In the most

recent study of the $A\,^3\Pi - X\,^3\Sigma^-$ transition of ND, Patel-Mishra *et al.*[58] recorded the $\Delta v = +1$ sequence bands using a molecular beam source. They combined their measurements with previous work on the 0–0, 1–1, and 2–2 bands[54–57] to extract equilibrium constants for the $A\,^3\Pi$ and $X\,^3\Sigma^-$ states of ND, although with a relatively large uncertainty. The $N = 1 \leftarrow 0$ transition of ND has also been measured recently by Saito and Goto[59] using submillimeter-wave spectroscopy, while the infrared vibration–rotation spectra have been measured by Ram and Bernath[60] by Fourier transform spectroscopy. In the FTS work, the rotational structure in several bands with vibrational levels up to $v = 6$ was measured, and molecular constants were reported for the ground state of ND.[60]

Although Boudjaadar *et al.*[52] measured the vibration–rotation bands of NH at high resolution, only relatively low J lines were measured. High J lines are essential, however, in determining higher-order constants such as D_v, H_v, and L_v for a light molecule like NH. These molecular constants are required for detecting NH at the high temperatures found in stellar atmospheres and flames.

In the present work, we have extended the NH vibration–rotation measurements to high J and combined them with the previously reported pure rotation lines,[33,46] vibration–rotation measurements,[48] and $A\,^3\Pi - X\,^3\Sigma^-$ lines[3] to extract an improved set of molecular constants. We have also recorded some NH vibration–rotation lines with the Phoenix spectrometer in order to check on the sensitivity and performance of a high-resolution cryogenic echelle spectrograph relative to an FTS. Although Phoenix was designed to look at weak astronomical sources, it may prove useful for ultrasensitive laboratory spectroscopy.

II. EXPERIMENT

A. Spectra recorded with a Fourier transform spectrometer

The infrared emission spectrum of NH have been observed in two experiments. In the first experiment, the vibration–rotation bands were observed as impurity during the search for CoN in a cobalt hollow cathode lamp using a discharge of 6 mTorr of N_2 Torr of Ne. The lamp was operated at 230 V and 330 mA current. In the second experiment, the NH bands were observed in a microwave discharge of a mixture of 200 mTorr of NH_3 and 2 Torr of He. Although the second spectrum was much cleaner than the first, lines in the 2200–2500 cm^{-1} region were stronger in the first spectrum. The emission from the discharge lamps was focused on the entrance aperture of the 1-m Fourier transform spectrometer associated with the McMath–Pierce telescope of the National Solar Observatory. The spectrometer was equipped with a CaF_2 beam splitter and liquid-nitrogen-cooled InSb detectors. The use of a Ge filter and InSb detectors limited the observation of the spectra to the 1800–5000 cm^{-1} spectral region. The spectra were recorded by coadding 8 and 20 scans, respectively, at a resolution of 0.02 cm^{-1}.

In the microwave-excited spectrum, in addition to the NH bands there were molecular lines of NH_3, the $w\,^1\Pi - a\,^1\Delta$ transition of N_2, and many atomic lines of He and N. This spectrum lacked strong impurity CO lines necessary for wave number calibration, so we decided to use strong atomic lines as transfer standards. For this purpose, we chose a separately recorded spectrum in which both CO and the atomic lines were strong. The atomic lines were first calibrated using the CO lines,[61] and then the calibration was transferred to the spectrum of NH. The spectra were measured using a program called PC-DECOMP developed at Kitt Peak. The NH vibration–rotation lines have been observed in our spectra with a maximum signal-to-noise ratio of about 15:1. The measurements of the strong and unblended lines are, therefore, expected to be accurate to ± 0.001 cm^{-1}. At higher N, the three spin components of each R branch line begin to merge. The three components are almost completely overlapped near the band head. The estimated uncertainty in the measurement of these broad lines is of the order of ± 0.003 cm^{-1}, and they have been given lower weights in the final fit.

In the 2240–2390 cm^{-1} spectral region, the lines of NH are overlapped by strong atmospheric CO_2 absorption, and some of the lines could not be measured. The NH lines near the edges of the CO_2 absorption features were also given lower weights in the final fit.

B. Spectra recorded with the cryogenic echelle spectrograph

Spectra were obtained by focusing the infrared emission from the microwave discharge with a 15 cm focal length CaF_2 lens into the input window of the Phoenix spectrograph. Phoenix is a cryogenic echelle spectrograph operated by Kitt Peak National Observatory and is designed primarily for use on nighttime telescopes. The instrument is operated at about 50 K to reduce thermal emission. An echelle grating is used in high order to obtain a compact high-resolution instrument that can be mounted at the Cassegrain focus of a telescope. The experimental conditions were similar to those used in the FTS experiments.

The Phoenix spectrograph employs refractive foreoptics to image an $f/15$ input onto a cold Lyot stop. At the Lyot stop, order sorting is performed by filters which limit the frequency bandpass to approximately one-half of the echelle free spectral range (~ 100 cm^{-1}). The filters are wedged to minimize fringing. Following the filters, refractive optics reimage the light onto the slit. The collimator and camera mirrors of the spectrograph are combined in a reflective Ritchey–Chretien system. Further details about the spectrograph can be found in Hinkle *et al.*[62] and on the National Optical Astronomy Observatory (NOAO) web site (www.noao.edu/kpno).

The detector is a 1024×1024 InSb array manufactured by Raytheon–Santa Barbara Research Center (SBRC). The array is a quadrant device and the array currently in use in Phoenix has two dead quadrants yielding, in essence, a 1024×512 array. Phoenix requires a 1024×216 pixel swath, with the long direction giving spectral information and the short direction giving spatial information. The pixels are 27 microns square. The read noise is 60 electrons and the dark current is 1 electron per pixel per s.

At the time of the observations, the performance of the spectrograph was limited by aberrations (coma) in the collimator. Coma smeared the image, both spatially and spectrally. The collimator was focused to give best spectral imaging which results in a line width about 3.6 pixels full width at half maximum (FWHM). This corresponds to a resolving power $R=\nu/\Delta\nu$ of 56 000. The microwave source filled the 4.4 mm long slit spatially. The coma degrades the spatial resolution as well, but in this application spatial resolution was not required. In the spatial direction, the FWHM of a point source is about 15 pixels.

Spectral coverage is limited by the length of the array, 1024 pixels, in the dispersion direction. Slight vignetting of the signal is present at the small wave number end of the spectra. A defect in the array at the small wave number end also reduces the spectral coverage by a few percent, about 100 pixels. The reciprocal dispersion of Phoenix is 5.0 $\times 10^{-4}$ cm^{-1}/micron at 3000 cm^{-1} on blaze (63.4 deg). The pixel size of 27 microns results in a single pixel covering 0.015 cm^{-1} near 3000 cm^{-1}. Typically, the bandwidth of the spectrum observed in one integration is about 0.47 percent (14 cm^{-1} at 3000 cm^{-1}).

The array does have pixel-to-pixel variation in both the sensitivity and dark current. To remove these, each observation involves at least three exposures, one of the source (''light''), one of the featureless ''flat'' (a *W* filament lamp), and a third ''dark'' exposure. Ideally, exposures with the source on (light) and off (dark) would be obtained, allowing cancellation of spectral features along the line of sight to the source (e.g., water vapor lines[63]). However, for many laboratory sources this is neither required nor practical.

An InSb array detector is similar in operation to a charge coupled device (CCD) in that photons cause charge separation and the electrons are then trapped in a potential well.[64] This charge is allowed to accumulate and is read periodically. The Aladdin array has a well depth of 100 000 electrons, which translates into 12 000 analog-to-digital unit (ADU) (1 ADU=8.3 electrons, where an ADU is the basic analog-to-digital unit used by the array controller software). The wells should not be allowed to fill to more than 80% (i.e., 10 000 ADU) of the full capacity.

For NH, the array was read every 60 s and a maximum of 3000 counts (ADUs) was measured. Two exposures were made of the same spectral region, and they were added together after reduction. The images were reduced to spectra by using the IRAF (Image Reduction and Analysis Facility) suite of programs available from NOAO. The ratio of (light−dark)/(flat−dark) was calculated to correct for the dark count and for pixel-to-pixel variations in sensitivity. Residual ''hot'' pixels were removed with an IRAF routine that replaces the signal level with an average of the values for nearby pixels. An 80-column-wide (spatial dimension) by 1024 long (spectral dimension) image was selected and converted by another IRAF routine into a spectrum, essentially by adding the 80 columns together. The detector had been carefully oriented to make this summation possible without additional image rotation. The first 100 pixels in the spectral dimension were discarded because of the defect at the edge of the array. The resulting spectrum appears as the upper panel of Fig. 1.

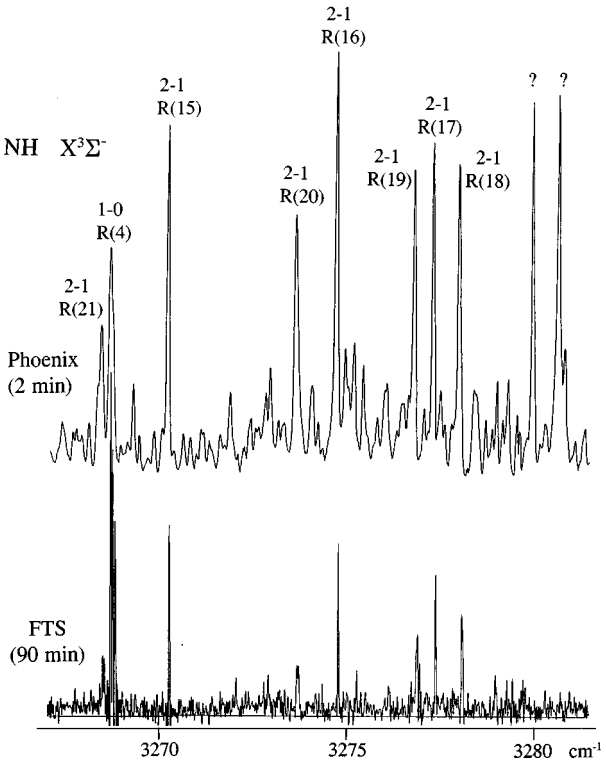

FIG. 1. A comparison of a part of the 2–1 band of NH near the *R* head recorded with Phoenix (upper trace) and the Fourier transform spectrometer (lower trace). The rotational lines have been marked with their N quantum numbers. The grassy features near the head are probably due to a larger molecule such as NH_2 or NH_3.

III. RESULTS AND DISCUSSION

Our spectrum consists of five vibration–rotation bands of NH in the $\Delta v=1$ sequence. Each band consists of three *R* and three *P* branches which can easily be recognized, particularly at lower N, by their characteristic triplet patterns. The triplet splitting in the *P* branch increases with increasing N, while in the *R* branch, this splitting decreases with increasing N values. The three components almost merge near the vibration–rotation head formed in the *R* branch. The *R* heads in the different bands are formed at relatively high N values; for example, in 1–0, 2–1, and 3–2 bands, the *R*-heads are at $R(N=19)$, $R(N=18)$, and $R(N=17)$, respectively. After the head, the returning lines again show signals of spin splitting, but only a small number of returning lines could be found because of their weak intensity. In general, the *P* lines are weaker in intensity than the *R* lines because of strong Herman–Wallis effects.[65]

We have extended the NH vibration–rotation measurements to include substantially higher N lines than those reported by Boudjaada *et al.*[52] For example, in the fundamental 1–0 band, we have measured lines up to $R(N=26)$ and $P(N=13)$ compared to $R(N=17)$ and $P(N=10)$ measured by Boudjaadar *et al.*[52] In the 2–1, 3–2, 4–3, and 5–4 bands, we have measured and fitted the lines up to $R(N)=25$, 23,

TABLE I. Spectroscopic constants (in cm^{-1}) for the $X\ ^3\Sigma^-$ state of NH. (*Note*: Numbers in parentheses are one standard deviation uncertainties in the last digits.)

Constants	$v=0$	$v=1$	$v=2$	$v=3$	$v=4$	$v=5$
T_v	0	3125.571 782(135)	6094.872 099(261)	8907.594 381(404)	11 562.315 424(660)	14 056.147 702(921)
B_v	16.343 272 27(345)	15.696 430 17(399)	15.050 538 14(835)	14.401 978 5(149)	13.745 873 3(191)	13.076 662 4(434)
$D_v\times10^3$	1.702 842 1(342)	1.679 474 8(275)	1.661 615 1(653)	1.649 965(131)	1.644 414(127)	1.660 696(603)
$H_v\times10^7$	1.238 29(113)	1.174 461(638)	1.110 79(174)	1.004 57(387)	0.710 44(225)	0.738 8(237)
$L_v\times10^{11}$	−1.459 8(146)	−1.454 04(462)	−1.694 6(146)	−1.838 4(359)	0	0
$M_v\times10^{16}$	7.190(644)	0	0	0	0	0
$\gamma_v\times10^2$	−5.486 37(102)	−5.178 41(137)	−4.882 10(248)	−4.583 27(397)	−4.257 71(626)	−3.963 28(926)
$\gamma_{Dv}\times10^5$	1.544 71(658)	1.402 54(397)	1.330 82(734)	1.226 4(126)	0.854 3(245)	1.203 8(837)
$\gamma_{Hv}\times10^9$	−1.438 0(895)	0	0	0	0	0
λ_v	0.919 893 0(248)	0.919 961(127)	0.918 447(243)	0.915 377(421)	0.911 319(630)	0.904 334(826)

18, and 12 compared to lines with $R(N)=14$, 12, 9, and 7 included in the analysis of Boudjaadar *et al.*[52] The observed line positions of NH vibration–rotation bands are available from PAPS[66] or from the authors upon request.

A part of the spectrum of 2–1 band near the *R*-head recorded with the Fourier transform spectrometer is also presented in Fig. 1 (lower panel) for comparison with the Phoenix spectrum. While comparing the two spectra, one must keep in mind that the FTS spectrum was coadded for 90 min while the Phoenix spectrum was obtained by summing two 1-min integrations using the same excitation source operated in similar conditions. As can be seen in Fig. 1, the NH molecular lines in the Phoenix spectrum have a better signal-to-noise ratio than those observed in the FTS spectrum. The grassy features observed near the 2–1 head are not noise since they are reproducible in each of the recorded scans. These lines are probably due to molecules like NH_2 or NH_3, although we have been unable to make specific assignments. The ground state ν_3 vibration of NH_2 and ν_2 vibration of NH_3 are expected to have transition in the same region. This observation suggests that the Phoenix spectrometer indeed has very high sensitivity.

The observed rotational lines of the individual bands were initially fitted separately using the customary $^3\Sigma^-$ Hamiltonian. An explicit listing of the matrix elements for the $^3\Sigma^-$ Hamiltonian is provided in our previous paper on NH[3]. In the final fit, however, the lines of all the bands were fitted simultaneously to provide a single set of constants for each vibrational level. In this fit, previous electronic measurements of the $A\ ^3\Pi-X\ ^3\Sigma^-$ transition of Brazier *et al.*,[3] vibration–rotation measurements of Bernath and Amano,[48] the zero field pure rotational wave numbers,[46] and solar pure rotation lines of Geller *et al.*[33] were also included. The combined data set was fitted with a standard deviation of 1.127. The weights for our vibration–rotation lines were chosen based on the signal-to-noise ratio and extent of blending, while the previous electronic, vibration–rotation, and pure rotation lines were weighted as claimed in the original papers. The rotational constants for different vibrational levels of the ground state have been provided in Table I. The constants of Table I were used to determine the equilibrium molecular constants for the ground state, which are provided in Table II. The equilibrium rotational constants of NH provide the ground-state equilibrium bond length of 1.037 186 0(19) Å, which is in excellent agreement with the previous values. The calculated dissociation energy D_0 of NH is 27 200 cm^{-1} (77.7 kcal/mole).[23] The observation of vibration rotation levels up to $v=5$ $N=12$ of NH, therefore, enable us to map more than half of the ground-state potential well.

It has been shown that a cryogenic grating spectrograph such as Phoenix should have a significant gain in sensitivity over an infrared spectrometer using an analog detector.[67] In Fig. 1, the signal-to-noise ratio (S/N) of the Phoenix spectrum with an integration time of 2 min is at least a factor of 3 greater than the signal-to-noise of the FTS spectrum with integration time of 90 min. Correcting for the difference in integration times (assuming that S/N grows as the square root of the integration time for both instruments), this naively implies that Phoenix is ~20 times more sensitive than the FTS. No attempt will be made to correct for the difference in resolution, which would further decrease the advantage of Phoenix. A meaningful comparison of sensitivities involves discussing some of the nuances of both instrumental approaches. As is well known to laboratory spectroscopists, the FTS technique is far superior to a grating spectrograph in many aspects other than sensitivity, and this also needs to be considered.

The sensitivity advantage of a cooled grating spectrograph, such as Phoenix, over an FTS is due to three factors: enhanced performance of InSb array detectors, a cold (nonthermally emissive) spectrograph, and a restricted bandpass. In astronomical applications, which are typically photon starved, sensitivity is the driving design goal. Phoenix was designed for nighttime astronomy applications. For many laboratory applications, unlike astronomical applications, the source can be made brighter or brought closer to the spectrograph. Hence, the gain from cooling the spec-

TABLE II. Main equilibrium constants (in cm^{-1}) for the $X\ ^3\Sigma^-$ state of NH. (*Note*: Numbers in parentheses are one standard deviation in the last digits.)

ω_e	3282.721 2(992)	α_e	0.650 379(173)
$\omega_e x_e$	79.041 5(798)	$\gamma_e\times10^3$	2.308(138)
$\omega_e y_e$	0.366 8(232)	$\delta_e\times10^4$	2.659(399)
$\omega_e z_e$	−0.051 57(217)	$\epsilon_e\times10^5$	4.348(375)
B_e	16.667 920 6(601)	r_e (Å)	1.037 186 0(19)

trograph is often minimal in many laboratory applications, since the internal thermal flux can be overwhelmed by source photons.

Similarly, it can be argued that restricting the bandpass of the FTS to match that of the dispersive spectrograph would improve the FTS S/N. For instance, the NH spectrum observed by Phoenix covered only 14 cm^{-1}, while the FTS spectrum covered the entire 1800–5000 cm^{-1} range. The signal-to-noise ratio in FTS spectra in the photon-noise limited case is inversely proportional to the square root of the bandwidth. If Phoenix were an FTS, this would account for a factor of 15 of Phoenix's sensitivity advantage. In reality, this gain is seldom achieved with an FTS because a filter as narrow as 14 cm^{-1} would probably result in detector-noise limited performance. In this case, the S/N becomes proportional to the source intensity, rather than the square root of the intensity. Also, for many applications a very restricted bandpass is undesirable since broader wave number coverage provides more information on the spectrum. Light molecules such as NH have very few lines in one setting of the grating. The section of spectrum displayed in Fig. 1 was carefully chosen to cover the 2–1 band head in order to increase the number of lines.

Since Phoenix is not an FTS, the bandwidth of interest is actually the bandwidth on a single detector pixel, ~0.015 cm^{-1}. The square root of the bandwidth factor of ~400 more than accounts for the sensitivity difference between the two instruments. The missing factor in the Phoenix performance is easily found in slit loss and other throughput losses. Hall *et al.*[68] found that the KPNO nighttime FTS had throughput of more than 50 percent. The throughput of Phoenix is ~13 percent before the slit loss is taken into account.

While an FTS is the ultimate broadband spectrograph, more advanced cryogenic spectrographs will provide much more extensive wave number coverage. Phoenix is a first-generation cooled grating spectrograph and is designed to image only one section of one echelle order in a single integration. Currently, much more coarsely ruled gratings are under development.[69] Future spectrographs employing these gratings will have a free spectral range matching the size of the array. In a spectrograph of this type, cross dispersion can be employed to map adjacent orders across the array, recording an extended section of spectrum on a two-dimensional array.

In the extreme photon-noise limited case of most laboratory experiments, the read noise and dark current of the array are of little significance. However, for some applications and, in particular, for nighttime astronomy, low detector noise is critical. With analog detectors, the signal-to-noise ratio (S/N) improves with the square root of the integration time. In an array detector, the spectrum is integrated on the array and, in the detector-noise limited case, the S/N improves linearly with the integration time. In addition, each pixel of the array has better performance characteristics than single-element InSb detectors.

Array-related gains in sensitivity are not easily gained back in an FTS. Placing an array detector in an FTS provides spatial coverage. The pixels at the FTS output port could be binned, but the advantage of the low noise in the small (27×27 micron) array pixels can be quickly lost if extraneous pixels are included in the sum. Also, infrared arrays are much more expensive than single-element detectors, and even though the cost increases only as the root of the number of pixels increases (approximately), it is clearly not cost effective to use a large array in a pixel binning application. Arrays are now made in standard sizes, with large arrays the optimum.

To use an array in integrating mode, an FTS would have to be operated in a step-and-integrate mode. Most FTSs operate in continuous scan mode, but both commercial and custom step scan instruments are available. In many laboratory experiments, however, the dominant source of noise is fluctuations in the source, for instance, in the strong atomic lines in a molecular emission experiment. In this case, the noise over the entire bandpass is seen by each pixel (''multiplex disadvantage''). The multiplex advantage of an FTS only applies when the dominant noise source is detector noise.

The disadvantages associated with dispersive spectrographs like Phoenix are well known. The wave number calibration of the spectrograph is the most serious problem. We have simply calibrated the NH lines seen by Phoenix with those from the FTS. Fortunately, the wave number scale of Phoenix is close to linear so that, in principle, two widely spaced lines are sufficient to calibrate the dispersion and thus, the absolute position of all the lines in each setting of the grating. Using calibration lines not present in the source (for example, lines from a hollow cathode calibration lamp) is generally not satisfactory in high-precision applications because the radiation from the lamp does not follow the same optical path as radiation from the source. The stable linear wave number scale of the FTS is an enormous advantage. An FTS still needs to be calibrated because the He–Ne laser and the radiation from the source are not exactly coincident but the shifts are very small (typically less than 0.01 cm^{-1}).

Both the operation and data reduction of dispersive spectrographs are different from that of the FTS. For an infrared device such as Phoenix, several exposures are required for each setting of the grating: a light, a dark, a flat, and perhaps a calibration source. These are familiar to observers with CCD grating systems in the visible, with the exception that dark exposures with the same integration time as the flat-field exposures are taken rather than bias frames.[63] When the grating setting is changed, the procedure must be repeated. Data reduction involves the manipulation of images using image reduction software such as IRAF or IDL. Systematic effects, rather than source or detector noise, can be a dominant noise source with a dispersive spectrograph. In contrast, an interferogram from an FTS requires phase correction and Fourier transformation to provide a spectrum. Removal of the system response in an FTS spectrum also requires a flat exposure.

At the moment, there is also a cost advantage in favor of the FTS. The budget for the construction of Phoenix was in excess of $2M and the detector alone costs over $100 000. Detector costs are decreasing and the current price for an Aladdin 1024×1024 InSb array detector from Raytheon is

becoming much more affordable if purchased through a foundry run. However, there is no intrinsic cost advantage of an FTS over a dispersive spectrograph. Phoenix is a novel, one-of-a-kind instrument with high engineering and construction costs. An FTS engineered and constructed in this same way would have similar costs.

An FTS also can easily achieve a resolution of about 0.002 cm^{-1} by using a longer (6 meter) optical path difference. Such high resolutions are at least an order of magnitude better than what is currently possible with an instrument like Phoenix. Since the resolution depends linearly on the grating size, and the grating in Phoenix is already large (a 200×400 cm *R2* echelle), increasing the resolution significantly is unlikely. The grating in a dispersive spectrograph can be double passed but the Phoenix design does not allow for this. In a laboratory instrument, this could easily be included in the design. The higher resolution (0.02 cm^{-1}) of the National Solar Observatory FTS can easily be seen in Fig. 1, where the resolution of Phoenix was about 0.05 cm^{-1}. The triplet fine structure of lines can be clearly seen in the FTS spectrum. Work is underway to improve the resolution of Phoenix to about 0.03 cm^{-1} at 3000 cm^{-1}.

In summary, the only advantage of a cryogenic grating spectrograph over the McMath–Pierce FTS for laboratory spectroscopy is sensitivity. The relative performance of Phoenix compared to an FTS improves at lower wave numbers where thermal emission increases, and for weaker signals. We see two applications for a cryogenic grating spectrograph in the laboratory environment. One application is in looking for very faint emission features of free radicals and ions. A second application is in spectroscopy of time-dependent chemical processes. An Aladdin 1024×1024 InSb array can be read out at $\sim$10 Hz. A single spectrum could be recorded in a much shorter integration time by use of a shutter mounted at the entrance to the Dewar. It should be possible to detect an emission line with an integrated flux at the Dewar entrance of a few $\times10^4$ photons.

IV. CONCLUSION

The emission spectra of five vibration–rotation bands 1–0, 2–1, 3–2, 4–3, and 5–4 of NH have been measured at high resolution using a Fourier transform spectrometer. These measurements have been combined with the previous $A\,^3\Pi-X\,^3\Sigma^-$ transition,[3] vibration–rotation,[48] pure rotation,[46] and solar[33] measurements to provide an improved set of rotational constants for the $v=0$, 1, 2, 3, 4 and 5 vibrational levels of the $X\,^3\Sigma^-$ state. The rotational constants for the individual vibrational levels have been used to evaluate improved equilibrium constants. NH spectra were also recorded with the new cryogenic echelle spectrograph called Phoenix. This instrument has higher sensitivity than a Fourier transform spectrometer and will be useful for the detection of faint laboratory spectra.

ACKNOWLEDGMENTS

We thank J. Wagner, C. Plymate and M. Dulick of the National Solar Observatory for assistance in obtaining the spectra. The Kitt Peak National Observatory and the National Solar Observatory are operated by the Association of Universities for Research in Astronomy, Inc., under contract with the National Science Foundation. The research described here was supported by funding from the NASA laboratory astrophysics program. Some support was also provided by the Natural Sciences and Engineering Research Council of Canada and the Petroleum Research Fund administered by the American Chemical Society.

[1] J. M. Eder, Denksch. Wien. Akad. **60**, 1 (1893).
[2] R. S. Ram and P. F. Bernath, J. Opt. Soc. Am. B **3**, 1170 (1986).
[3] C. R. Brazier, R. S. Ram, and P. F. Bernath, J. Mol. Spectrosc. **120**, 381 (1986).
[4] I. Tokue and Y. Ito, Chem. Phys. **79**, 383 (1983); **89**, 51 (1984).
[5] I. Tokue and Fujimaki, J. Phys. Chem. **88**, 6250 (1984).
[6] H. K. Haak and F. Stuhl, J. Phys. Chem. **88**, 2201 (1984); **88**, 3627 (1984).
[7] U. Blumenstein, F. Rohrer, and F. Stuhl, Chem. Phys. Lett. **107**, 347 (1984).
[8] W. H. Smith, J. Brzozowski, and P. Erman, J. Chem. Phys. **64**, 4628 (1976).
[9] D. R. Johnson and J. W. Hudgens, J. Chem. Phys. **92**, 6420 (1990).
[10] M. N. R. Ashford, S. G. Clement, J. D. Howe, and C. M. Western, J. Chem. Soc., Faraday Trans. **87**, 2515 (1991).
[11] S. G. Clement, M. N. R. Ashford, and C. M. Western, J. Chem. Soc., Faraday Trans. **88**, 3121 (1992).
[12] S. G. Clement, M. N. R. Ashford, C. M. Western, R. D. Johnson, and J. W. Hudgens, J. Chem. Phys. **96**, 5538 (1992).
[13] S. G. Clement, M. N. R. Ashford, C. M. Clement, E. de Beer, C. A. de Lange, and N. P. C. Westwood, J. Chem. Phys. **96**, 4963 (1992).
[14] M. Hawley, A. P. Baronavski, and H. N. Nelson, J. Chem. Phys. **99**, 2638 (1993).
[15] N. P. L. Wales, E. de Beer, N. P. C. Westwood, W. J. Buma, C. A. de Lange, and M. C. van Hemert, J. Chem. Phys. **100**, 7984 (1994).
[16] M. Rohrig and H. G. Wagner, J. Mol. Struct. **349**, 285 (1995).
[17] K. P. Kirby and E. M. Goldfield, J. Chem. Phys. **94**, 1271 (1991).
[18] G. Parlant, P. J. Dagdigian, and D. R. Yarkony, J. Chem. Phys. **94**, 2364 (1991).
[19] J. K. Park and H. Sun, Chem. Phys. Lett. **211**, 618 (1993).
[20] G. Jansen, B. A. Hess, and C. M. Marian, J. Phys. Chem. **97**, 10011 (1993).
[21] J. Ischtwan and M. A. Collins, J. Chem. Phys. **100**, 8080 (1994).
[22] J. Seong, J. K. Park, and H. Sun, Chem. Phys. Lett. **228**, 443 (1994).
[23] J. Espinosa-Garcia, J. C. Corchado, J. Fernandez, and A. Marquez, Chem. Phys. Lett. **233**, 220 (1995).
[24] R. W. Shaw, Astrophys. J. **83**, 225 (1936).
[25] P. Swings, C. T. Elvey, and H. W. Babcock, Astrophys. J. **94**, 320 (1941).
[26] J. L. Schmitt, Publ. Astron. Soc. Pac. **81**, 657 (1969).
[27] D. L. Lambert and R. Beer, Astrophys. J. **177**, 541 (1972).
[28] M. M. Litvak and E. N. Rodriguez Kuiper, Astrophys. J. **253**, 622 (1982).
[29] D. L. Lambert, J. A. Brown, K. H. Hinkle, and H. R. Johnson, Astron. J. **283**, 223 (1984).
[30] D. L. Lambert, B. Gustafsson, K. Erikson, and K. H. Hinkle, Astrophys. J., Suppl. Ser. **62**, 373 (1986).
[31] S. T. Ridgway, D. F. Carbon, D. N. B. Hall, and J. Jewell, Astrophys. J., Suppl. Ser. **54**, 177 (1984).
[32] N. Grevesse, D. L. Lambert, A. J. Sauval, C. E. van Dishoeck, C. B. Farmer, and R. H. Norton, Astron. Astrophys. **232**, 225 (1990).
[33] M. Gellar, A. J. Sauval, N. Grevesse, C. B. Farmer, and R. H. Norton, Astron. Astrophys. **249**, 550 (1991).
[34] D. M. Meyer and K. C. Roth, Astrophys. J. Lett. **376**, L49 (1991).
[35] A. W. Brewer, P. A. Davis, and J. B. Kerr, Nature (London) **240**, 35 (1972).
[36] J. A. Miller, M. C. Branch, and R. J. Kee, Combust. Flame **43**, 81 (1981).
[37] W. R. Anderson, L. J. Deker, and A. J. Kotlar, Combust. Flame **48**, 179 (1982).
[38] M. S. Chou, A. M. Dean, and D. Stern, J. Chem. Phys. **76**, 5334 (1982).
[39] C. Y. R. Wu, J. Chem. Phys. **86**, 5584 (1987).
[40] A. Hofzumahaus and F. Stuhl, J. Chem. Phys. **82**, 3152 (1985); **82**, 5519 (1985).
[41] D. Patel-Misra, G. Parlant, D. G. Sander, D. R. Yarkony, and P. J. Dagdigian, J. Chem. Phys. **94**, 1913 (1991).

[42] B. Bohn, F. Stuhl, G. Parlant, P. J. Dagdigian, and D. R. Yarkony, J. Chem. Phys. **96**, 5059 (1992).
[43] A. Dreizler, T. Dreizler, and J. Wolfrum, J. Mol. Struct. **349**, 285 (1995).
[44] H. E. Radford and M. M. Litvak, Chem. Phys. Lett. **34**, 561 (1975).
[45] F. D. Wayne and H. E. Radford, Mol. Phys. **32**, 1407 (1976).
[46] F. C. Van Der Huevel, W. L. Meerts, and A. Dymanus, Chem. Phys. Lett. **92**, 215 (1982).
[47] T. Klaus, S. Takano, and G. Winnewisser, Astron. Astrophys. **322**, L1 (1997).
[48] P. F. Bernath and T. Amano, J. Mol. Spectrosc. **95**, 359 (1982).
[49] D. E. Milligan and M. E. Jacox, J. Chem. Phys. **41**, 2838 (1964).
[50] H. Sakai, P. Hansen, M. Esplin, R. Johansson, M. Peltola, and J. Strong, Appl. Opt. **21**, 228 (1982).
[51] B. D. Geen and G. E. Caledonia, J. Chem. Phys. **77**, 3821 (1982).
[52] D. Boudjaadar, J. Brion, P. Chollet, G. Guelachvili, and M. Verloet, J. Mol. Spectrosc. **119**, 352 (1986).
[53] I. Marino and K. Kawaguchi, J. Mol. Spectrosc. **182**, 428 (1997).
[54] M. Shimauchi, Sci. Light (Tokyo) **15**, 161 (1966).
[55] M. Shimauchi, Sci. Light (Tokyo) **16**, 185 (1967).
[56] I. Kopp, M. Kronvist, and N. Åslund, Ark. Fys. **30**, 9 (1965).
[57] P. Bollmark, I. Kopp, and B. Rydh, J. Mol. Spectrosc. **34**, 487 (1970).
[58] D. Patel-Misra, D. G. Sauder, and P. J. Dagdigian, Chem. Phys. Lett. **174**, 113 (1990).
[59] S. Saito and M. Goto, Astrophys. J. Lett. **410**, L53 (1993).
[60] R. S. Ram and P. F. Bernsth, J. Mol. Spectrosc. **176**, 329 (1996).
[61] A. G. Maki and J. S. Wells, *Wavenumber Calibration Tables from Heterodyne Frequency Measurements*, NIST Special Publication 821 (U.S. Government Printing Office, Washington, DC, 1991).
[62] K. H. Hinkle, R. Cuberly, N. Gaughan, J. Heynssens, R. R. Joyce, S. Ridgway, P. Schmitt, and J. E. Simmons, Proc. SPIE **3354**, 810 (1998).
[63] R. R. Joyce, ''Observing with Infrared Arrays,'' in *Astronomical CCD Observing and Reduction Techniques*, edited by S. Howell, ASP Conference Series Vol. 23 (1992), p. 258.
[64] G. H. Reiche, *Detection of Light: From the Ultraviolet to the Submillimeter* (Cambridge University Press, Cambridge, 1994).
[65] C. Chackerian, G. Guelachvili, A. Lopez-Pineiro, and R. H. Tipping, J. Chem. Phys. **90**, 641 (1989).
[66] See AIP Document No. PAPS JCPSA6-110-014912 for nine pages of data tables. Order by PAPS number and journal reference from American Institute of Physics, Physics Auxiliary Publication Service, 500 Sunnyside Boulevard, Woodbury, New York 11797-2999, Fax: 516-576-2223, e-mail: paps@aip.org. The price is $1.50 for each microfiche (98 pages) or $5.00 for photocopies of up to 30 pages and $0.15 for each additional page over 30 pages. Airmail additional. Make checks payable to the American Institute of Physics.
[67] S. T. Ridgway and K. H. Hinkle, ''Strategies for Very High Resolution Infrared Spectroscopy,'' in *High Resolution Spectroscopy with the VLT*, edited by M.-H. Ulrich (ESO Conference and Workshop Proceedings 40) 1993) (European Southern Observatory, Garching, Germany), p. 213.
[68] D. N. B. Hall, S. T. Ridgway, E. A. Bell, and J. M. Yarborough, Proc. Soc. Photo-Opt. Instrum. Eng. **172**, 121 (1979).
[69] P. J. Kuzmenko and D. R. Ciarlo, Proc. SPIE **3354**, 357 (1998).